

PAPER • OPEN ACCESS

SOC Estimation of Lithium Battery Based on Dual Adaptive Extended Kalman Filter

To cite this article: Yongliang Zheng *et al* 2019 *IOP Conf. Ser.: Mater. Sci. Eng.* **677** 032077

View the [article online](#) for updates and enhancements.



240th ECS Meeting

Oct 10-14, 2021, Orlando, Florida

**Register early and save
up to 20% on registration costs**

Early registration deadline Sep 13

REGISTER NOW



SOC Estimation of Lithium Battery Based on Dual Adaptive Extended Kalman Filter

Yongliang Zheng*, Feng He^a, and Wenliang Wang^b

School of mechanical engineering, Guizhou University, Guiyang, Guizhou, 550025, China

*Corresponding author: 964646197@qq.com, ^a fenghe-01@vip.sina.com,

^b 1091010676@qq.com

Abstract. The estimation accuracy of single extended Kalman filter is not high, also it is affected by the initial value of state of charge (SOC). The second-order RC equivalent circuit model of lithium battery is established, and a joint algorithm, dual extended Kalman filter (DEKF) is proposed. Besides, the covariance matching theory is introduced for DEKF under the complex condition of uncertain noise statistical characteristics to improve the estimation accuracy. The improved DEKF is compared with another joint algorithms, i.e. recursive least squares and extended Kalman filter (RLS-EKF). Through the validation of battery test data, the modified dual extended Kalman filter based on covariance adaptive algorithm can realize real-time online estimation of battery SOC and time-varying parameters, and the estimation accuracy of lithium battery SOC and battery time-varying parameters is higher.

Key words: State of Charge; Dual Extended Kalman Filter; Recursive Least Square Algorithms; Online Estimation

1. Introduction

The estimation of SOC is the key to battery management system (BMS). Common SOC estimation methods are: ampere-hour counting method, impedance method, open circuit voltage method (OCV), neural network, support vector machine (SVM) and Kalman filter (KF) estimation method. The ampere hour counting method is affected by the process noise of the battery operation and the instrument observation noise, so the error accumulates with time; the impedance method and OCV are constrained by time setting, so they are not suitable for power battery SOC prediction; SVM and neural network are subject to sample richness and hardware limitations, there are certain limitations in the application of the current stage. Kalman filter algorithm based on empirical battery model and equivalent circuit model (ECM), due to low computational complexity and accurate modeling, using optimized autoregressive processing characteristics, has great advantages of SOC estimation in power batteries [1-2]. Nonlinear Kalman filtering such as extended Kalman filtering, unscented Kalman filtering or Kalman filtering modified by artificial intelligence algorithms have been widely used in SOC estimation and have achieved good prediction effects [3-6]. When the traditional single Kalman filter estimates SOC, battery resistances is regarded as a constant, ignoring the fact that the internal resistance of the battery change during operations, so cannot accurately reflect the SOC change of the battery. Recently, many ECM-



based battery SOC estimation studies, combined with multiple estimation methods, so they can identify more battery parameters and lay the foundation for other battery state predictions. In order to achieve battery SOC and SOH estimation, Andre et al. [7] introduced KF-UKF to predict the SOC and time-varying parameters of the battery, and the predicted result as the input of SVM to realize SOH prediction, but the SVM prediction is completed in offline state, also, a lot of sample training is needed. Xiong et al. [8] used multi-time scale dual extended Kalman filter (DEKF) for capacity estimation of different aging stages of batteries, but only considering the first-order RC battery model. Nikolaos et al. [9] proposed that DEKF estimates SOC and battery parameters in different dynamic loads and SOH stages. Compared with simple EKF, the accuracy of SOC estimation has been improved to some extent.

Aiming at the shortcomings of traditional Kalman filtering on battery SOC prediction, a second-order RC ECM of lithium battery is established. An improved DEKF based on covariance matching theory is proposed to predict the SOC and identify the time-varying parameters of lithium battery. Finally, it compares with RLS-EKF using the estimation accuracy of battery SOC and battery parameters under different conditions.

2. Battery Model Establishment

An accurate battery model is the premise of Kalman filter to estimate the state of the battery, and the second-order RC ECM can more accurately reflect the dynamic changes of lithium battery than the first-order RC model, PNGV and DP model [10]. Therefore, a second-order RC ECM is employed shown in Fig. 1.

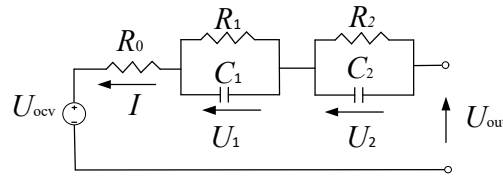


Figure 1. Second order RC ECM

In Fig.1, I is the current, R_0 is the ohmic resistance, C_1 and R_1 are the electrochemical polarization capacitance and resistance, and C_2 and R_2 are the concentration polarization capacitance and resistance, and U_{ocv} and U_{out} are the open circuit voltage and the terminal voltage, respectively. The battery ECM is represented by equation (1):

$$\begin{cases} \dot{U}_1 = \frac{1}{R_1 C_1} U_1 + \frac{1}{C_1} I \\ \dot{U}_2 = \frac{1}{R_2 C_2} U_2 + \frac{1}{C_2} I \\ U_{out} = U_{ocv} - U_1 - U_2 - IR_0 \end{cases} \quad (1)$$

The definition of SOC can be expressed:

$$SOC(t) = SOC_0 - \frac{\eta I \Delta t}{C_p} \quad (2)$$

Where η is the coulombic efficiency, this paper takes 1, SOC_0 is the initial value, sampling time $\Delta t = 1s$, C_p is the actual capacity of the battery.

Discretize equation (1) and combine equation (2) to obtain the equation of state of battery.

$$\mathbf{x}_{k+1} = \begin{bmatrix} 1 & 0 & 0 \\ 0 & e^{-\frac{\Delta t}{R_1 C_1}} & 0 \\ 0 & 0 & e^{-\frac{\Delta t}{R_2 C_2}} \end{bmatrix} \mathbf{x}_k + \begin{bmatrix} -\Delta t / C_p \\ R_1 (1 - e^{-\frac{\Delta t}{R_1 C_1}}) \\ R_2 (1 - e^{-\frac{\Delta t}{R_2 C_2}}) \end{bmatrix} \times I_k \quad (3)$$

$$U_{out,k} = U_{ocv}(\text{SOC}_k) - U_{1,k} - U_{2,k} - I_k R_0 \quad (4)$$

Where, the state vector $\mathbf{x}_k = [\text{SOC}_k, U_{1,k}, U_{2,k}]^T$, the time constant $\tau_1 = R_1 C_1$ and $\tau_2 = R_2 C_2$, the open circuit voltage U_{ocv} can be obtained by fitting the relationship with the SOC, and dynamic changes of lithium batteries are expressed by formulas (3) and (4).

3. Joint Estimation Algorithms

3.1. Double Extended Kalman Filter

In order to simultaneously realize the online estimation of battery SOC and time-varying parameters, we designed two extended Kalman filters running in parallel. The first filter is used to estimate SOC and the other is used for the identification of battery time-varying parameters. The setting of the battery model process noise and the initial value of the measurement noise greatly influence the estimation accuracy of the SOC, hence the extended Kalman filter for SOC estimation is improved by the covariance matching theory.

The extended Kalman filter for estimating the SOC obtains the state and measurement equation of the battery SOC, respectively, according to equations (3) and (4):

$$\mathbf{x}_{k+1} = f(\mathbf{x}_k, u_k) + \mathbf{w}_k^x \quad (5)$$

$$\mathbf{y}_k = g(\mathbf{x}_k, u_k) + v_k^x \quad (6)$$

Where, output $\mathbf{y}_k = U_{out,k}$, control variable $u_k = I_k$, process noise $\mathbf{w}_k^x \sim N(0, \mathbf{Q}^x)$ and observed noise $v_k^x \sim N(0, R^x)$.

The Jacobian matrix of state is obtained:

$$\hat{A}_k = \left. \frac{\partial f(\mathbf{x}_k, u_k)}{\partial \mathbf{x}_k} \right|_{\mathbf{x}_k = \hat{\mathbf{x}}_k^+} = \begin{bmatrix} 1 & 0 & 0 \\ 0 & e^{-\frac{\Delta t}{R_1 C_1}} & 0 \\ 0 & 0 & e^{-\frac{\Delta t}{R_2 C_2}} \end{bmatrix} \quad (7)$$

$$\hat{H}_k^x = \left. \frac{\partial g(\mathbf{x}_k, u_k)}{\partial \mathbf{x}_k} \right|_{\mathbf{x}_k = \hat{\mathbf{x}}_k^-} = [\partial U_{ocv} / \partial \text{SOC}_k, -1, -1] \quad (8)$$

After the SOC estimation is completed, the SOC becomes a known input, and another extended Kalman filter can estimate the time-varying parameter θ of the battery. Based on equations (5) and (6), the state and observation equation of θ are obtained:

$$\theta_{k+1} = \theta_k + \mathbf{w}_k^\theta \quad (9)$$

$$\mathbf{y}_k = g(\mathbf{x}_k, u_k, \theta_k) + v_k^\theta \quad (10)$$

Where, the time-varying parameter $\theta_k = [R_0, R_1, C_1, R_2, C_2]^T$, the process noise $\mathbf{w}_k^\theta \sim N(0, \mathbf{Q}^\theta)$, and the observed noise $v_k^\theta \sim N(0, R^\theta)$.

The Jacobian matrix of the battery time-varying parameter is expressed as:

$$\hat{H}_k^\theta = \left. \frac{dg(\hat{x}_{k+1}^-, u_{k+1}, \theta)}{d\theta} \right|_{\theta=\hat{\theta}_{k+1}^-} = \frac{\partial g(\hat{x}_{k+1}^-, u_{k+1}, \theta)}{\partial \theta} + \frac{\partial g(\hat{x}_{k+1}^-, u_{k+1}, \theta)}{\partial \hat{x}_{k+1}^-} \frac{d\hat{x}_{k+1}^-}{d\theta} \quad (11)$$

The dual adaptive extended Kalman filter (DAEKF) realization process is shown in Fig. 2(a):

Step 1: Initialize \mathbf{x}_0 , \mathbf{Q}_0 , \mathbf{R}_0 , \mathbf{P}_0 ; θ_0 , \mathbf{Q}_0^θ , \mathbf{R}_0^θ , \mathbf{P}_0^θ .

Step 2: θ time-update equations

$$\begin{aligned} \hat{\theta}_{k+1}^- &= \hat{\theta}_k^+ \\ \mathbf{P}_{\theta, k+1}^- &= \mathbf{P}_{\theta, k}^+ + \mathbf{Q}_k^\theta \end{aligned} \quad (12)$$

Step 3: \mathbf{x} time-update equations

$$\begin{aligned} \hat{\mathbf{x}}_{k+1}^- &= f(\hat{\mathbf{x}}_k^+, u_k, \hat{\theta}_{k+1}^-) \\ \mathbf{P}_{x, k+1}^- &= \hat{A}_k \mathbf{P}_{x, k}^+ \hat{A}_k^T + \mathbf{Q}_k^x \end{aligned} \quad (13)$$

Step 4: \mathbf{x} measurement-update equations

$$\begin{aligned} \mathbf{K}_k^x &= \mathbf{P}_{x, k+1}^- (\hat{H}_k^x)^T (\hat{H}_k^x \mathbf{P}_{x, k+1}^- (\hat{H}_k^x)^T + \mathbf{R}_k^x)^{-1} \\ \hat{\mathbf{x}}_{k+1}^+ &= \hat{\mathbf{x}}_{k+1}^- + \mathbf{K}_k^x (y_k - \hat{y}_k) \\ \mathbf{P}_{x, k+1}^+ &= (\mathbf{I} - \mathbf{K}_k^x \hat{H}_k^x) \mathbf{P}_{x, k+1}^- \end{aligned} \quad (14)$$

Step 5: Adaptive Covariance Matching

$$\begin{aligned} \mathbf{B}_k &= \frac{1}{M} \sum_{i=k-M+1}^k (y_k - \hat{y}_k)_i (y_k - \hat{y}_k)_i^T \\ \mathbf{Q}_{k+1}^x &= \mathbf{K}_k^x \mathbf{B}_k (\mathbf{K}_k^x)^T \\ \mathbf{R}_{k+1}^x &= \mathbf{B}_k - \hat{H}_k^x \mathbf{P}_{x, k+1}^- (\hat{H}_k^x)^T \end{aligned} \quad (15)$$

Where M is the window size, $M=100$.

Step 6: θ measurement-update equations

$$\begin{aligned} \mathbf{K}_k^\theta &= \mathbf{P}_{\theta, k+1}^- (\hat{H}_k^\theta)^T (\hat{H}_k^\theta \mathbf{P}_{\theta, k+1}^- (\hat{H}_k^\theta)^T + \mathbf{R}_k^\theta)^{-1} \\ \hat{\theta}_{k+1}^+ &= \hat{\theta}_{k+1}^- + \mathbf{K}_k^\theta (y_k - \hat{y}_k) \\ \mathbf{P}_{\theta, k+1}^+ &= (\mathbf{I} - \mathbf{K}_k^\theta \hat{H}_k^\theta) \mathbf{P}_{\theta, k+1}^- \end{aligned} \quad (16)$$

3.2. RLS-EKF Joint Estimation Algorithm

The recursive least squares algorithm (RLS) has a simple structure and a small amount of computation, and it is suitable for online identification of battery time-varying parameters [11-12]. The following is the derivation of RLS.

Convert equation (1)

$$L(s) = \frac{U_{ocv}(s) - U_{out}(s)}{I(s)} = (R_0 + \frac{R_1}{1 + \tau_1 s} + \frac{R_2}{1 + \tau_2 s}) = \frac{R_0 s^2 + \frac{1}{\tau_1 \tau_2} (R_0 \tau_1 + R_0 \tau_2 + R_1 \tau_2 + R_2 \tau_1) s + \frac{R_0 + R_1 + R_2}{\tau_1 \tau_2}}{s^2 + [s(\tau_1 + \tau_2) + 1] / \tau_1 \tau_2} \quad (17)$$

Convert equation (17)

$$v_k = b_1 v_{k-1} + b_2 v_{k-2} + b_3 I_k + b_4 I_{k-1} + b_5 I_{k-2} \quad (18)$$

Where b_1 , b_2 , b_3 , b_4 , b_5 are constants correlative to the time-varying parameters of the battery, expressed as follows:

$$\begin{cases} R_0 = \frac{b_3 - b_4 + b_5}{1 + b_1 - b_2}, \tau_1 \tau_2 = \frac{T^2(1 + b_1 - b_2)}{4(1 - b_1 - b_2)}, \tau_1 + \tau_2 = \frac{T(1 + b_2)}{(1 - b_1 - b_2)}, R_0 \tau_1 + R_0 \tau_2 + R_1 \tau_2 + R_2 \tau_1 = \frac{T(b_3 - b_5)}{(1 - b_1 - b_2)} \\ R_0 + R_1 + R_2 = \frac{b_3 + b_4 + b_5}{(1 - b_1 - b_2)} \end{cases}$$

In order to speed up the convergence, the forgetting factor is introduced, and the RLS with the forgetting factor λ is obtained:

$$v_k = U_{ocv}(SOC_k) - U_{out,k} \quad (19)$$

$$e_k = (v_k - \Psi^T(k) \hat{\epsilon}(k)) \quad (20)$$

$$K(k) = \frac{P(k-1) \Psi^T(k)}{\lambda + \Psi^T(k) P(k-1) \Psi(k)} \quad (21)$$

$$P(k) = \frac{1}{\lambda} (I - K(k) \Psi^T(k)) P(k-1) \quad (22)$$

$$\hat{\epsilon}(k) = \hat{\epsilon}(k-1) + K(k) e(k) \quad (23)$$

Where, $e(k)$ is the prediction error, $P(k)$ is the covariance matrix, $K(k)$ is the gain, $\Psi(k) = [v_{k-1}, v_{k-2}, I_k, I_{k-1}, I_{k-2}]^T$, $\epsilon = [b_1, b_2, b_3, b_4, b_5]^T$, $0.95 < \lambda < 1$.

By combining with the EKF for SOC estimation, RLS-EKF can realize simultaneously online estimation of battery SOC and time-varying parameters, which is good for enhancing the accuracy of SOC estimation. The RLS-EKF structure diagram is shown in Fig. 2(b):

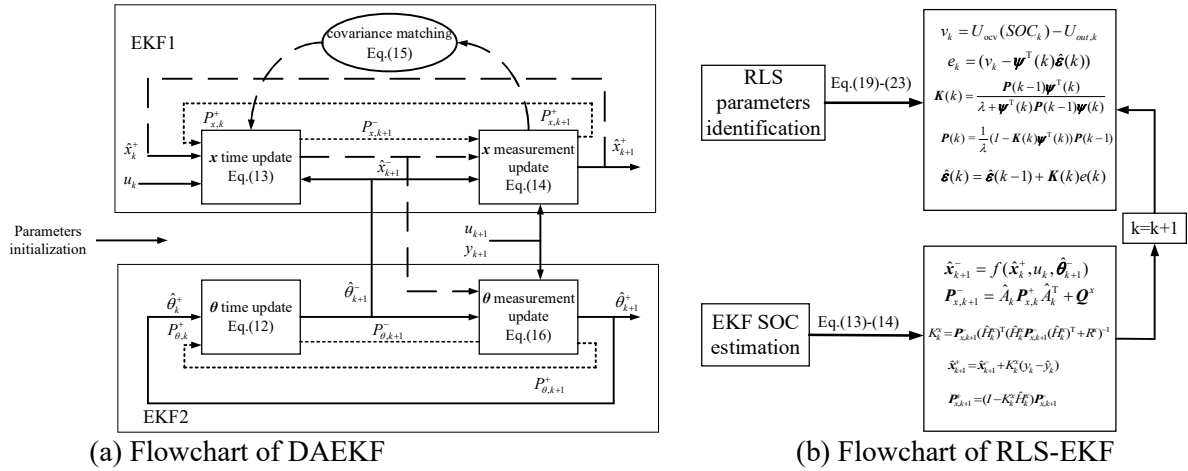


Figure 2. Flowchart of joint algorithms

4. Test Verification

The accuracy of the joint estimation algorithms for SOC and time-varying parameters can be verified by battery data as shown in Table 1[13].

Table 1. Battery parameters

Rated capacity	2000mAh	Upper / lower limit cutoff voltage	4.2V/2.5V
Rated voltage	3.6V	Test temperature	25°C

4.1. Model Accuracy Verification

The accuracy of the established second-order RC ECM is reflected by the comparison between the voltage comparison. In Fig. 3 (a), in the dynamic stress test conditions (DST), the model voltage is not

much different from the actual voltage. In Fig. 3 (b), the maximum absolute voltage error is 68mV, the voltage average relative error (MRE) is 3.9mV, and the voltage root mean square error (RMSE) is 6.1mV, so the model accuracy meets the requirements.

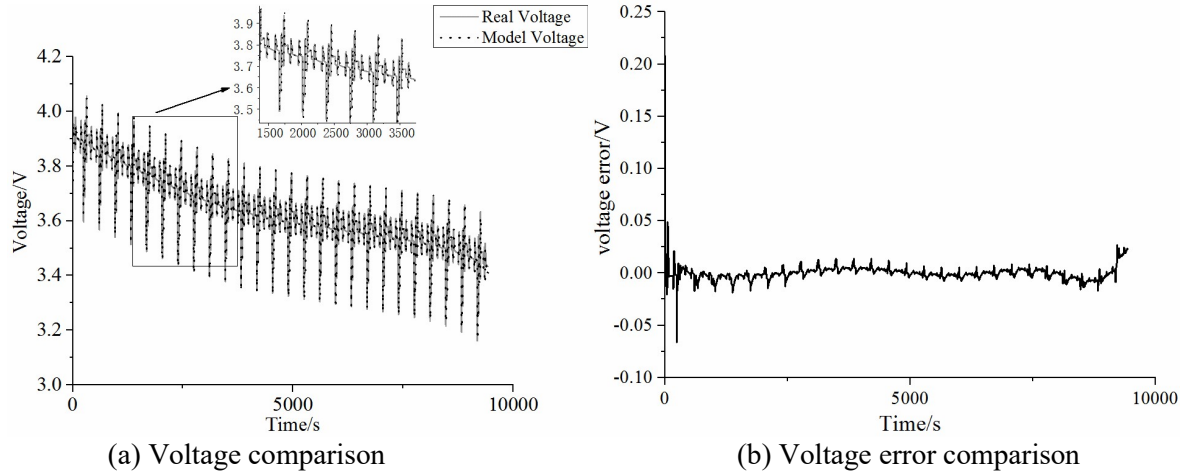


Figure 3. Voltage comparison under DST

4.2. SOC Estimation Verification

The joint algorithms of SOC estimation are verified by dynamic stress test conditions (DST), and Beijing Dynamic Pressure Test Conditions (BJDST). All are done at 25 °C.

Fig. 4 (a) is the comparison performed under DST with a true SOC initial value of 0.8 and an initial SOC value of 0.6 for each algorithm. It can be seen from Fig. 4 (a) and (b) that all three algorithms can track the real SOC, and DAEKF reaches the convergence phase at the earliest. The MRE of DAEKF, EKF and RLS-EKF are 0.81%, 2.60% and 0.97%, respectively, and their RMSE are 0.92%, 2.69%, and 1.20%, respectively, reflecting the advantages of the joint algorithms in SOC estimation.

Fig. 6 (a) and (b) show the SOC and SOC error comparisons under BJDST. Under this condition, the convergence speed of RLS-EKF is slower than the other two, whereas DAEKF converges faster. The EKF has the largest error, its MRE and RMSE are 2.60% and 2.67%, respectively; the MRE of the RLS-EKF is 1.90%, but the RMSE is 3.01%, and the MRE and RMSE of the DAEKF are 0.88% and 0.95%, respectively.

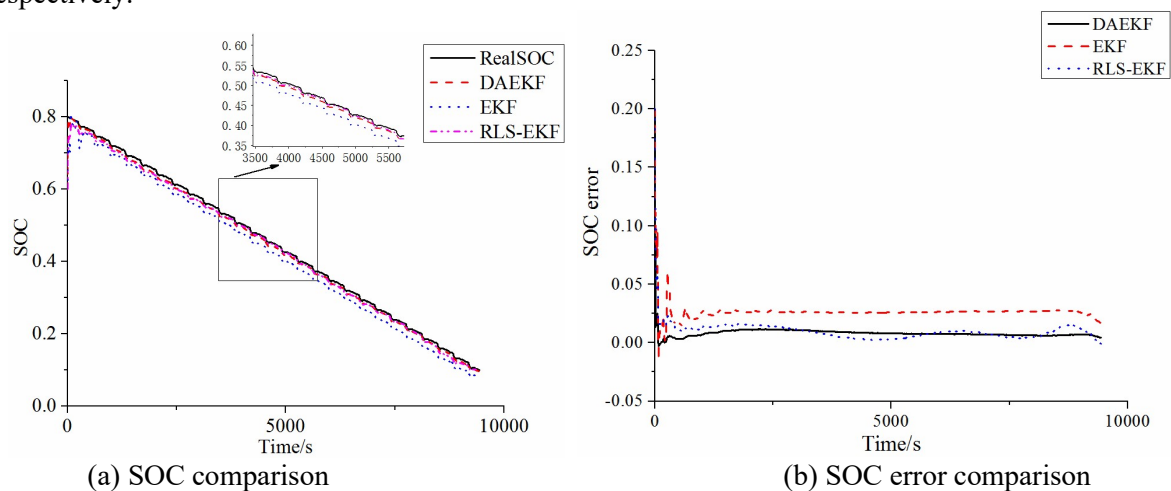


Figure 4. SOC comparison under DST

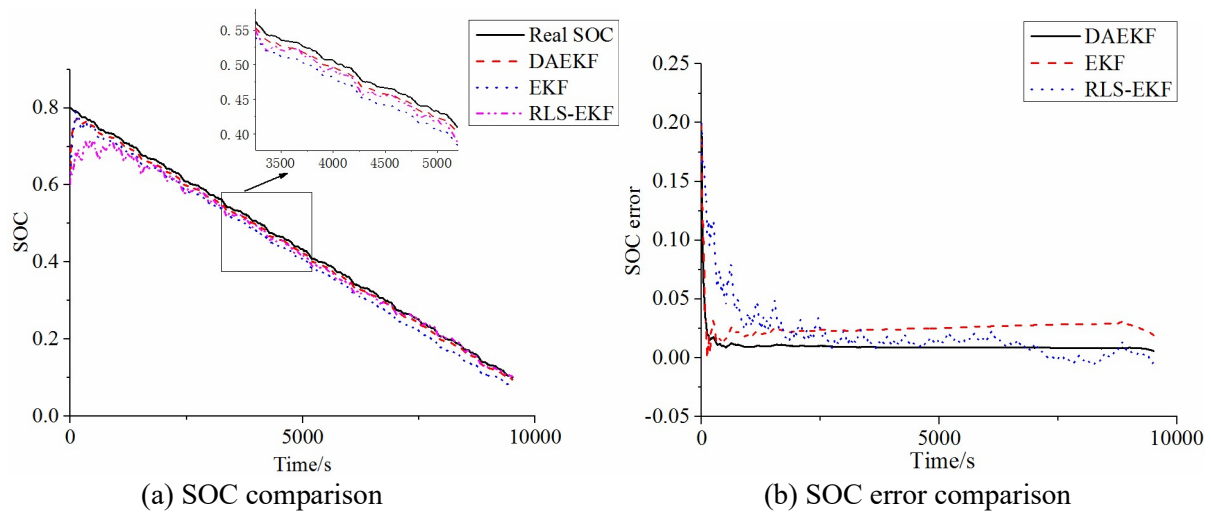


Figure 5. SOC comparison under BJDST

4.3. Time-varying Parameter Estimation Verification

In the BJDST, both the DAEKF and RLS-EKF algorithms have an initial value of R_0 of 0.11Ω and the reference value is 0.08Ω . In Fig.6 (a), the DAEKF algorithm converges faster than the RLS-EKF, with an RMSE of 0.0034Ω , while the R_0 estimated by the RLS-EKF fluctuates greatly at the beginning, with an amplitude of 0.44Ω and an RMSE of 0.0184Ω . In the DST of Fig.6 (b), the initial value of R_0 of each algorithm is set to 0.02Ω . Similarly, the R_0 estimated by the DAEKF algorithm quickly enters the convergence phase, the RMSE is 0.0026Ω , while the maximum fluctuation amplitude of the RLS-EKF is 0.36Ω , and its RMSE is 0.0136Ω .

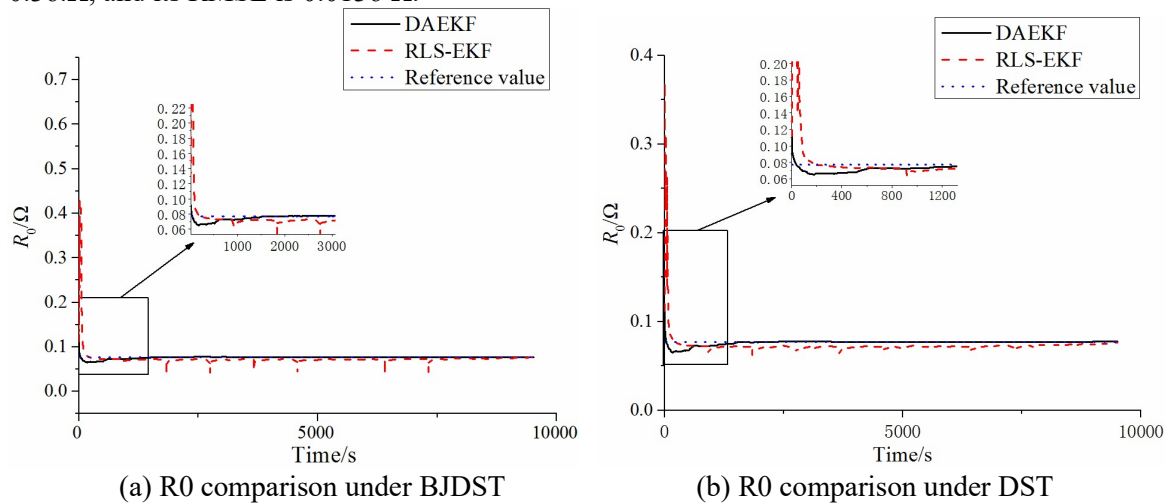


Figure 6. R_0 estimation comparison

5. Conclusion

(1) The established second-order RC ECM accurately reflects the dynamic changes of the battery. The error of voltage and actual voltage of the established second-order RC ECM does not exceed 70mV, which satisfies the requirements.

(2) The joint estimation algorithms for realizing online estimation of time-varying parameters of the battery have higher estimation accuracy. Considering that the battery parameters change during the working process, two joint algorithms, DAEKF and RLS-EKF, are established. Thanks to the ability to estimate battery internal resistance online, the estimation accuracies of SOC by the joint algorithms in different working conditions are higher than that by the traditional single extended Kalman filter.

(3) The convergence speed and estimation accuracy of DAEKF in SOC and internal resistance estimation are better than RLS-EKF. The DAEKF with covariance matching theory solves the influence of unknown noise on the estimation accuracy, and the estimation error of SOC and internal resistance is within 1% and 0.0034Ω , respectively, which can accurately estimate the SOC and time-varying parameters of the battery.

Acknowledgments

This study was supported by Guizhou province science and technology support projects ([2018]2178).

References

- [1] Wei Z, Zhao J, Zou C, et al. Comparative study of methods for integrated model identification and state of charge estimation of lithium-ion battery [J]. *Journal of Power Sources*, 2018, 402:189-197.
- [2] Limei Wang, Dong Lu, Qiang Liu et al. State of charge estimation for LiFePO₄ battery via dual extended kalman filter and charging voltage curve [J]. *Electrochimica Acta* 296 (2019) 1009-1017.
- [3] XIE Yong-dong, HE Zhi-gang, CHEN Dong. SOC estimation of power battery based on AUK [J]. *Journal of Beijing Jiaotong University*, 2018, 198(02): 135-143.
- [4] Xie Changjun, Fei Yalong, Zeng Chunnian, et al. State-of-Charge Estimation of Lithium-Ion Battery Using Unscented Particle Filter in Vehicle[J]. *Transactions of China Electrotechnical Society*, 2018 (1): 3958-3964.
- [5] XIANG Yu, MA Xiao-jun, LIU Chun-guang. Estimation of Model Parameters and SOC of Lithium Batteries Based on IPSO-EKF[J]. *Acta Armamentarii*, 2014, 35(10):1659-1666.
- [6] LIU Zhengyu, TANG Wei, WANG Xuesong, et al. Cell SOC Estimation of Battery Packs Based on Dual Time-Scale EKPF [J]. *China Mechanical Engineering*, 2018, v.29; No.495(15):74-79.
- [7] ANDRE D, Appel C, Soczka-Guth T, et al. Advanced mathematical methods of SOC and SOH estimation for lithium-ion batteries[J]. *Journal of Power Sources*, 2013, 224(none):20–27.
- [8] R. Xiong, F. Sun, Z. Chen, et al, A data-driven multi-scale extended Kalman filtering based parameter and state estimation approach of lithium-ion olymer battery in electric vehicles, *Applied Energy*, 113 (2014) 463–476
- [9] NIKOLAOS W, Jörn A, Alexander F, et al. Revisiting the dual extended Kalman filter for battery state-of-charge and state-of-health estimation: A use-case life cycle analysis [J]. *Journal of Energy Storage*, 2018, 19:73-87.
- [10] Prashant Shrivastava, Tey Kok Soon, Mohd Yamani Idna Bin Idris, et al. Overview of model-based online state-of-charge estimation using Kalman filter family for lithium-ion batteries[J]. *Renewable and Sustainable Energy Reviews*, 2019, 113:109-233.
- [11] Tong S, Klein M P, Park J W. On-line optimization of battery open circuit voltage for improved state-of-charge and state-of-health estimation [J]. *Journal of Power Sources*, 2015, 293:416-428.
- [12] WEI J, DONG G, CHEN Z. On-board adaptive model for state of charge estimation of lithium-ion batteries based on Kalman filter with proportional integral-based error adjustment[J]. *Journal of Power Sources*, 2017, 365:308-319.
- [13] Zheng F, Xing Y, Jiang J, et al. Influence of different open circuit voltage tests on state of charge online estimation for lithium-ion batteries [J]. *Applied Energy*, 2016, 183:513-525.